Role of Terrain Preview in Energy Management of Hybrid Electric Vehicles

Chen Zhang, Ardalan Vahidi, *Member, IEEE*, Pierluigi Pisu, *Member, IEEE*, Xiaopeng Li, and Keith Tennant

***Abstract*—Energy-management strategy plays a critical role in high fuel economy that modern hybrid electric vehicles can achieve, yet a lack of information about future driving conditions is one of the limitations of fulfilling the maximum fuel economy potential of hybrid vehicles. Today, with wider deployment of vehicle telematic technologies, prediction of future driving conditions, e.g., road grade, is becoming more realistic. This paper evaluates the potential gain in fuel economy if road grade information is integrated into the energy management of hybrid vehicles. Real-world road geometry information is utilized in power-management decisions by using both dynamic programming (DP) and a standard equivalent consumption minimization strategy (ECMS). At the same time, two baseline control strategies with no future information are developed and validated for comparison purposes. Simulation results show that road terrain preview enables fuel savings. The level of improvement depends on the cruising speed, control strategy, road profile, and the size of the battery.**

***Index Terms*—Energy management, hybrid electric vehicle, road grade, terrain preview.**

I. Introduction

TODAY'S hybrid electric vehicles (HEVs) have much better fuel economy than conventional nonhybrid vehicles. The improved fuel economy is mainly due to the use of extra battery energy storage and one or more electric machines that assist the combustion engine by providing additional power, therefore allowing the use of a smaller combustion engine operating under more fuel-efficient conditions. Battery storage also provides a buffer that enables capturing the braking energy that is normally wasted as heat. The extra degree of freedom provided by the auxiliary power source enables substantial improvements in fuel efficiency, as demonstrated by commercially available HEVs, yet the added efficiency of any HEV is dependent on the power-management strategy (PMS), which determines the split of power request between the combustion engine and the electric drive [22].

Most PMSs in production vehicles operate based on logical "if–then–else" type rules and preoptimized maps and rely only on instantaneous power demand and state of the vehicle [4], [5], [8], [22]. In search of an optimal (or suboptimal) solution, many researchers have formulated the PMS as a fuel-minimization problem over a driving cycle.

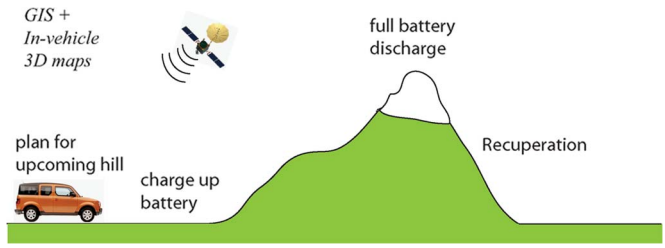

Fig. 1. Schematic of predictive energy management based on 3-D terrain maps.

This optimal control problem can be solved by numerical dynamic programming (DP), assuming full or statistical knowledge of the future driving cycle [10], [13]. Because of its dependence on future driving cycle and its large computational burden, DP is not suitable for online use and is considered only as a benchmark for the best achievable fuel economy [13]. Instead, to obtain a suboptimal solution, the global optimization problem is simplified to an instantaneous one in the family of equivalent consumption minimization strategy (ECMS) methods [12], [14], [16], [20]. In ECMS methods, the battery charging/discharging at each instant is translated to the equivalent fuel gained/used, and the sum of instantaneous actual and equivalent fueling rate is minimized. ECMS methods are computationally efficient; however, their performance may vary, depending on the cycle because of lack of information about the upcoming driving cycle.

The truly optimal PMS depends on the future driving conditions. Knowledge of upcoming terrain and traffic conditions will help more judicious use of the electric power by extending the planning horizon. Such information can now become available, as illustrated in Fig. 1, by combined use of a vehicle-navigation system, 3-D road maps, and even possibly radioed traffic information. Research on the use of preview road information for improving the fuel economy of commercial heavy trucks with conventional powertrains has been done in the past [9]. Look-ahead use of traffic and traffic signal information has been proposed as a means to predict future velocity profile [7] or reduce rapid accelerations and decelerations, which helps fuel economy [2], [11]. While there is the belief among HEV experts that preview terrain information can increase the fuel efficiency of hybrid vehicles, the amount of possible improvement to fuel economy has not clearly been explored in the literature [10], [18], nor is there a systematic methodology to utilize such preview knowledge in existing PMSs. The adaptive

Manuscript received June 30, 2009; revised October 9, 2009. First published December 18, 2009; current version published March 19, 2010. This work was supported by research grants from Intermap Technologies and the U.S. Army Tank Automotive Research, Development, and Engineering Center. The review of this paper was coordinated by Prof. J. Hur.

C. Zhang, A. Vahidi, and P. Pisu are with the Department of Mechanical Engineering, Clemson University, Clemson, SC 29634 USA (e-mail: chenz@clemson.edu; avahidi@clemson.edu; pisup@clemson.edu).

X. Li and K. Tennant are with the Intermap Technology Corporation, Ottawa, ON K2E 1A2, Canada.

Color versions of one or more of the figures in this paper are available online at http://ieeexplore.ieee.org.

Digital Object Identifier 10.1109/TVT.2009.2038707

TABLE I
SPECIFICATION OF A PARALLEL HEV FOR SIMULATION

maximum engine power	120kw	maximum motor power	45kw
battery capacity C	5.5 Ah	battery voltage	312V
reducer ratio	2	final drive ratio	10.5

ECMS [16] and telemetry ECMS [19] power-management algorithms aim to use past and partial future information to adjust their tuning parameter, respectively. However, none explores knowledge of future terrain information.

In contrast to the past research, the main purpose of this paper is to quantify the potentials of 3-D road terrain maps to improve the fuel economy of a parallel hybrid vehicle. In the present study, we decouple the influence of velocity variation by focusing on constant-velocity cruise situations. The future road terrain can be determined using in-vehicle 3-D maps and vehicle GPS-based navigation. In this paper, we use real-world 3-D aerial maps created by Intermap Technologies. The digital elevation maps and orthorectified radar images are gathered using a proprietary airborne interferometric synthetic aperture radar technology from a fixed-wing aircraft.

Section II presents the vehicle configuration and its model for simulation. Section III summarizes seven road terrain profiles, in which three are simulated arc terrains and the other four are real terrain profiles from the California mountain area. In Section IV, the energy-management strategies with and without preview are presented. Section V evaluates the impact of terrain preview on fuel economy based on several simulation results. Section VI concludes this paper with a summary of our observations.

II. HYBRID ELECTRIC VEHICLE POWERTRAIN CONFIGURATION AND MODEL

A midsize 2000-kg passenger vehicle with a parallel hybrid electric configuration is selected for this study. Parameter values and detailed performance maps for various powertrain components were extracted from the database of the Powertrain System Analysis Toolkit (PSAT) simulation software developed by Argonne National Laboratory [1]. A 120-kW gasoline internal combustion engine and a 45-kW ac motor are arranged in a pretransmission configuration and connected to a five-speed automatic transmission via a clutch and a torque coupler. The key vehicle parameters are summarized in Table I.

The PSAT-based full-order powertrain model contains the vehicle velocity, clutch input speed, and battery state of charge (SOC) as its dynamic states with many other lookup tables and logical switches. Maintaining this level of complexity for developing and evaluating an optimal power-management scheme is neither practical nor necessary. In fact, the only state critical in power management is the slowly varying SOC of the battery [21]. Therefore, a reduced-order model is developed, which contains the battery SOC as its only dynamic state. The battery is modeled, with its open-circuit voltage in series with a constant internal resistance. SOC dynamics are described by

$$\frac{d}{dt}SOC = -\frac{V_{\rm oc} - \sqrt{V_{\rm oc}^2 - 4P_{\rm batt}R}}{2RC} \tag{1}$$

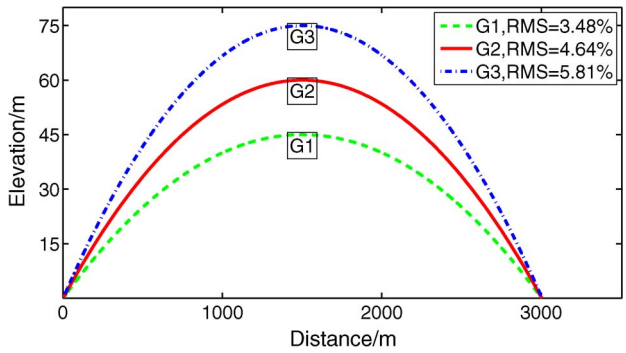

Fig. 2. Simulated arc terrain elevation profiles G1–G3 and their root-mean-square grade values.

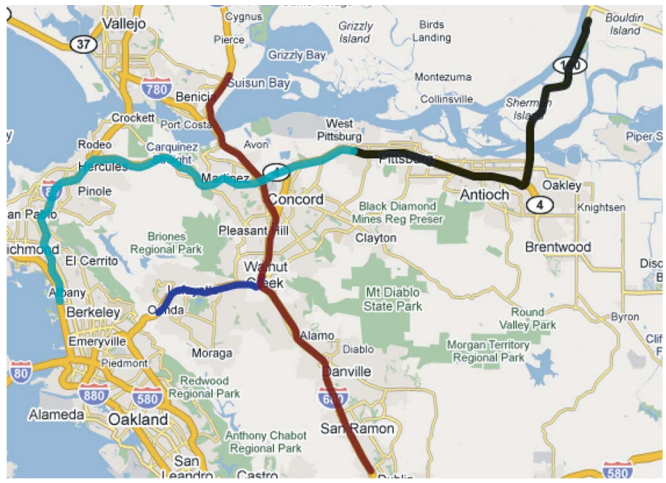

Fig. 3. Google Map view of terrain G4–G7 in Contra Costa county, CA.

where $V_{\rm oc}$ is the open-circuit voltage of the battery, $P_{\rm batt}$ is the electric power at the battery output side, R is the internal resistance of the battery and connecting wires, and C is the battery capacitance. More details can be found in [17]. In the reduced-order model, we continue to use lookup tables from PSAT to model the engine fuel rate and motor losses. The fuel rate $\dot{m}_f$ is mapped from the engine torque $T_{\rm eng}$ and engine speed $\omega_{\rm eng}$

$$\dot{m}_f = f(T_{\rm eng}, \omega_{\rm eng}). \tag{2}$$

Another lookup table is used to relate the motor mechanical power P_m to motor speed ω_m and output electrical power of the battery $P_{\rm batt}$, which is given by

$$P_{\rm batt} = g(P_m, \omega_m). \tag{3}$$

The gear-shifting strategy, which depends on wheel torque demand and vehicle velocity, is also adopted from PSAT and implemented as a lookup map.

III. TEST ROAD PROFILES

Two sets of road-elevation profiles are used for this study. The first is a set of three simulated arc terrains with the same span but different peak elevations and maximum grades; Fig. 2 shows their profiles. The second is a set of four real-world road profiles selected from Intermap's 3-D terrain map

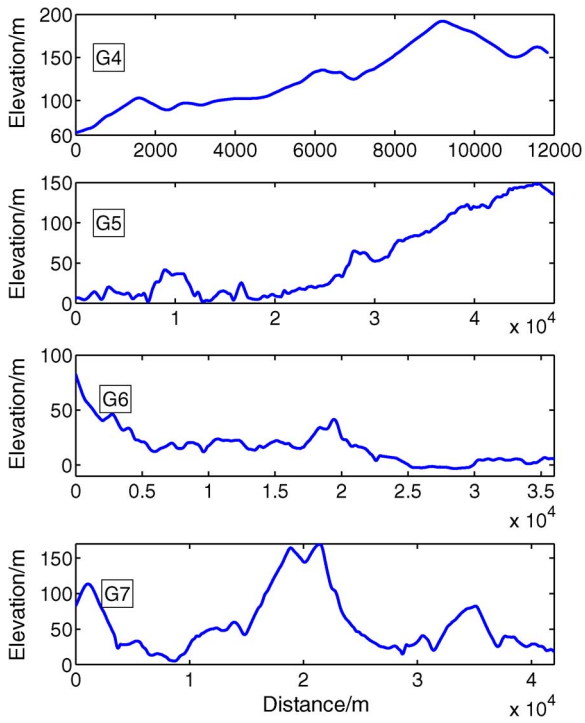

Fig. 4. Elevation profiles of real-world terrains G4–G7.

TABLE II
STATISTICS OF THE TERRAIN DATA

route	length (km)	mean (%)	max (%)	min (%)	RMS (%)
G4	12	0.77	4.02	-3.73	2.1877
G5	48	0.26	4.72	-3.73	1.32
G6	36	-0.21	2.96	-4.33	1.04
G7	48	-0.17	5.32	-7.97	2.31

database. Fig. 3 shows a Google Map[1] of this region in Contra Costa county, CA. Intermap's road geometry database has the information stored as 3-D road vectors with accurate longitude, latitude, and altitude. This information is postprocessed and converted to 2-D information, in which slope is a function of distance along the road. Fig. 4 shows the elevation profile for each of these roads. The statistical information of the grades, including maximum and minimum road slope and the slope root-mean-square values, are listed in Table II.

In this paper, the focus is on realizing fuel economy gains with road grade preview only. To decouple the influence of unknown future velocity, we assume that the vehicle is traveling with a constant and known cruise speed. The case with varying speed requires further investigation and is planned as a next step of this work. With the known speed assumption, upcoming slopes will be known as a function of time.

IV. POWER-MANAGEMENT STRATEGY

The supervisory control unit of an HEV determines the power or torque split ratio between the combustion engine and the electric motor aiming to reduce fuel use. This section describes the structure of two types of PMSs used in this work: 1) strategies that determine the baseline achievable fuel economy without terrain preview and 2) strategies with terrain preview. Finding a "fair" baseline PMS, i.e., one that is near optimal in the absence of preview, was one of the main challenges of this research. We have considered both a rule-based (RB) and a modified ECMS method as baseline strategies without preview. When terrain preview is available, we use both ECMS and DP to determine the best achievable fuel economy. The details of each algorithm are described next.

[1]Google Maps is a registered trademark of Google Inc.

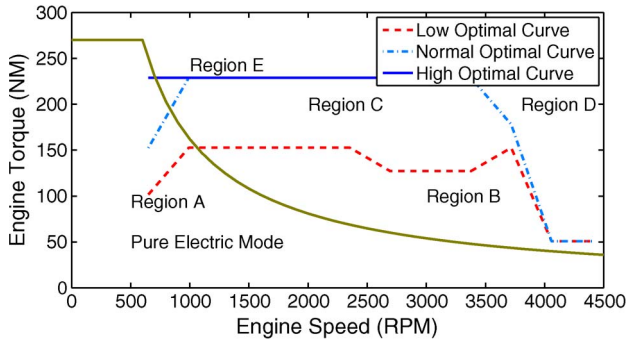

Fig. 5. Schematic of different operating regions imposed by an RB PMS.

A. RB Control Strategy

An RB power-management scheme is considered first, because such RB strategies are most widely used in current hybrid vehicles. Examples of different RB strategies can be found in research papers as well [8], [13], [15]. We adopt the structure of the RB strategy used in PSAT, which could achieve good fuel economies for most tested cycles. To increase the fuel economy, the rules are designed to turn off the engine at low power demands and run it near statically optimized operating lines when on.

In this RB strategy, the desired charging or discharging power of the battery $P_{\mathrm{batt\_dmd}}$ is calculated as a static function of the battery's SOC, SOC. A positive $P_{\mathrm{batt\_dmd}}$ denotes charging, and a negative value means discharging power. The driver's power request $P_{\mathrm{drv\_dmd}}$ is inferred from the accelerator pedal position (or through a driver model in simulations). The sum of the driver and battery power demands determines the total power demand P_{dmd}

$$P_{\mathrm{dmd}} = P_{\mathrm{drv\_dmd}} + P_{\mathrm{batt\_dmd}} \tag{4}$$

from which the total torque demand T_{dmd} at the torque coupler is calculated by dividing the known engine speed.[2] A statically optimized map, along with a set of rules, is used to determine the engine and motor torques. Fig. 5 shows a schematic of this map partitioned into five different regions by statically optimized curves. In this figure, the *normal optimal curve* T_{opt} represents the most efficient operating line of the engine as a function of the engine speed. However, operating the engine on this line does not necessarily result in minimum fuel use. In other words, the most efficient way to run the engine is not always equivalent to the most efficient way to run the hybrid powertrain. This is due to electrical losses that need to be accounted

[2]The vehicle speed is known, and the transmission status is also external to the RB controller and is known. Therefore, the engine speed can be calculated.

for in the calculation of engine best operating points (OPs). In the RB approach, two additional curves, i.e., the *high optimal curve* $T_{\text{opt\_hi}}$ and the *low optimal curve* $T_{\text{opt\_lo}}$, are also calculated, which allow operating the engine higher or lower such that overall efficiency is increased. Five rules are used.

1) At very low torque levels, when $(\omega_{\text{eng}}, T_{\text{dmd}})$ is in region A, running the engine is not efficient; the engine is turned off $(T_{\text{eng}} = 0)$, and the motor drives (brakes) the vehicle $(T_{\text{mot}} = T_{\text{dmd}})$.
2) When $(\omega_{\text{eng}}, T_{\text{dmd}})$ is in region B, the engine is run on the low optimal line $(T_{\text{eng}} = T_{\text{opt\_lo}})$, and the excess torque is used to charge the battery, i.e., $(T_{\text{mot}} = T_{\text{dmd}} - T_{\text{opt\_lo}})$.
3) When $(\omega_{\text{eng}}, T_{\text{dmd}})$ is in region C, the engine is run on the normal optimal line $(T_{\text{eng}} = T_{\text{opt}})$, and $(T_{\text{mot}} = T_{\text{dmd}} - T_{\text{opt\_hi}})$.
4) When $(\omega_{\text{eng}}, T_{\text{dmd}})$ is in region D, the engine is run on the high optimal line $(T_{\text{eng}} = T_{\text{opt\_hi}})$, and $(T_{\text{mot}} = T_{\text{dmd}} - T_{\text{opt\_hi}})$.
5) At very high torque levels, when $(\omega_{\text{eng}}, T_{\text{dmd}})$ is in region E, the engine cannot meet the torque demand, the engine is run on the high optimal line $(T_{\text{eng}} = T_{\text{opt\_hi}})$, and the motor supplies the rest $(T_{\text{mot}} = T_{\text{dmd}} - T_{\text{opt\_hi}})$.

Since it is difficult to systematically incorporate future information in the RB strategy, it is only treated as a baseline strategy without preview.

B. Optimal Control Strategy: ECMS

Maximizing the fuel economy of a HEV can explicitly be formulated as minimization of the cost function [8]

$$J_f = \int_{t_0}^{t_f} \dot{m}_f(t,u)\,dt + \phi(SOC_i, SOC_f) \tag{5}$$

subject to the powertrain model equations and the following constraints:

$$\begin{aligned} SOC_{\min} \le SOC \le SOC_{\max} \\ T_{\text{eng}}^{\min}(\omega_{\text{eng}}) \le T_{\text{eng}}(\omega_{\text{eng}}) \le T_{\text{eng}}^{\max}(\omega_{\text{eng}}) \\ T_m^{\min}(\omega_m) \le T_m(\omega_m) \le T_m^{\max}(\omega_m) \end{aligned} \tag{6}$$

where $\dot{m}_f$ is the fuel consumption rate; the control law u is the power split ratio; SOC_i and SOC_f are the initial SOC and final SOC, respectively; $SOC_{\min}$ and $SOC_{\max}$ are the minimum and maximum bounds on SOC; $T_{\text{eng}}^{\min}(\omega_{\text{eng}})$ and $T_{\text{eng}}^{\max}(\omega_{\text{eng}})$ are the minimum and maximum torque of the engine at a given speed; $T_m^{\min}(\omega_m)$ and $T_m^{\max}(\omega_m)$ are the minimum and maximum torque of the electric motor at a given speed; and $\phi(SOC_i, SOC_f)$ is the penalty function (which is also referred to as equivalent fuel consumption) for the deviation of the final SOC from its initial value. The final SOC is usually constrained to be equal to the initial SOC; in that case, $\phi(SOC_i, SOC_f)$ will vanish.

Analytical solutions to this optimization problem do not exist in general, due to its many state and input constraints, nonlinearities, and its dependence on future power demands.

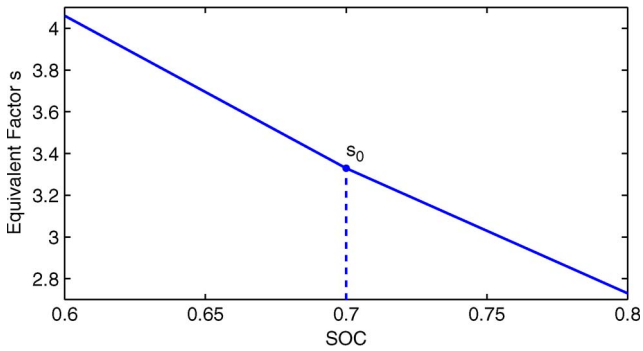

Fig. 6. Equivalent factor s as function of SOC; $s_0 = \sqrt{s_{\text{dis}} s_{\text{chg}}}$.

In the ECMS, the preceding optimization problem is simplified to minimization of the *instantaneous* (rather than integral) equivalent fuel rate $\dot{m}_{f,\text{equ}}$, as shown in [15]

$$\dot{m}_{f,\text{equ}} = \dot{m}_f + s \cdot P_e / H_l \tag{7}$$

where P_e is the net power charged to the battery or the power drawn, including the power loss to the internal resistance, and H_l is the low heating value of the fuel.

1) ECMS Without Preview: Choice of the fuel equivalence factor s is important and critical to the fuel economy and charge sustenance of the battery. Its true value is a function of future power demands, which are unknown in the absence of preview. Several methods were proposed to estimate s [12], [16], [20]. In [8], average charging and discharging efficiencies are used to approximate the value of s as follows:

$$s = \begin{cases} s_{\text{dis}}, & P_e(t,u) > 0 \\ s_{\text{chg}}, & P_e(t,u) < 0 \end{cases}$$

where

$$s_{\text{dis}} = \frac{1}{\bar{\eta}_e^{(d)} \bar{\eta}_f} \tag{8}$$

$$s_{\text{chg}} = \frac{\bar{\eta}_e^{(c)}}{\bar{\eta}_f}. \tag{9}$$

Here, $\bar{\eta}_e^{(d)}$ and $\bar{\eta}_e^{(c)}$ are the average electric circuit efficiencies for discharge and charge, respectively, and $\bar{\eta}_f$ is the average efficiency for the combustion engine.

Because this choice of s is not a function of the battery's SOC, the SOC may deviate far from its desired value. Inspired by the approach in [20], in our baseline ECMS (BL ECMS), we modify s as a function of the SOC based on the bilinear relationship shown in Fig. 6. The values of s_{chg} and s_{dis} are determined using (8) and (9) based on assumed average efficiencies and without using preview.

In addition, we enforce two additional rules to ensure that the SOC does not exceed its limits.

1) If $SOC > SOC_{\max}$, charge mode is not allowed.
2) If $SOC < SOC_{\min}$, discharge mode is not allowed.

$SOC_{\max}$ and $SOC_{\min}$ are set to 0.8 and 0.6, respectively, in our study, which is consistent with the bounds enforced in practice.

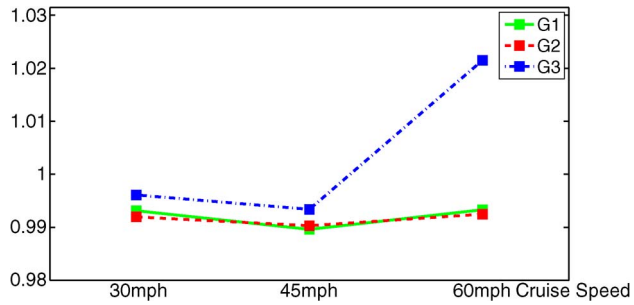

Fig. 7. Fuel economy gains with DP and ECMS, both with terrain preview. The y-axis shows the ratio between the fuel economies with DP and standard preview ECMS.

2) ECMS With Preview: With known future power demands, it is possible to find the true value for the equivalence factor s. It can be shown that the value of s that results in minimum fuel use and renders $SOC_f = SOC_0$ is a constant [6] on the following conditions.

1) The SOC constraint in (6) is relaxed.
2) The right-hand side of SOC dynamics (1) is not an explicit function of SOC.

We use a numerical procedure that iterates to find the constant value of s with known future power demands at the beginning of each driving cycle. Specifically, in this process, a constant s is initially guessed, and the optimization is carried out based on this initial value of s. The resulting final SOC SOC_f is then compared with the desired value SOC_0. If it is different, the value of s is updated based on a bisectional search, and the process is repeated until finally, $SOC_f = SOC_0$.

C. Optimal Control Strategy-DP

When the future power demands are known, the optimal power-split ratio that minimizes the cost function (5) subject to the model equation and constraints in (6) can numerically be obtained using DP [13]. The time horizon, the state variable SOC, and the control variables are discretized, and the optimal control problem is solved backward in time according to Bellman's principle of optimality. Details of DP can be found in [3].

In simulations, we observed little difference between the results of DP and those of ECMS with preview. To see the difference between DP and ECMS with preview, the fuel economies of the two control strategies are compared, as shown in Fig. 7, for simulated grades G1, G2, and G3 and for cruise speeds of 30, 45, and 60 mi/h. It can be seen that, in most cases, the difference is less that 1%, and the largest difference is about 2%. The difference could be due to linear approximation and discretization errors in DP, which may make DP deviate from the true optimal solution. Another potential factor for the difference is that the SOC trajectory in standard ECMS is allowed to go over its constraints, whereas DP enforces the SOC constraints. However, this factor was not the case for simulations in Fig. 7.

Therefore, for the sake of reducing computational burden, in the rest of the simulations in this paper, standard ECMS is considered to be control strategy with preview, unless SOC constraint in ECMS is violated; in that case, the DP result will be used.

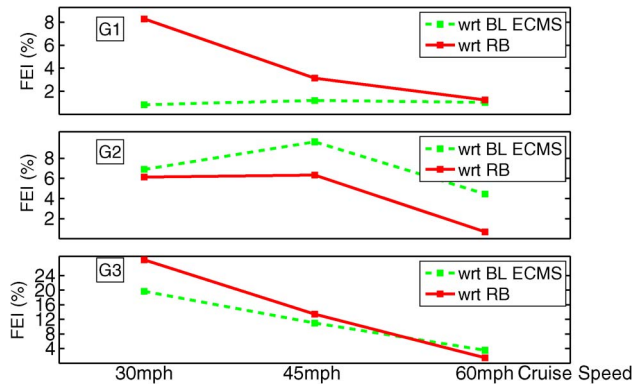

Fig. 8. FEI of arc terrains w.r.t. BL ECMS and the RB strategy.

V. Simulation Analysis

To determine the impact of terrain preview on fuel economy, we compare the fuel economy obtained via ECMS with preview (or DP with preview) to that obtained via ECMS and the RB strategy without preview. The RB strategy without preview is representative of the industry approach, and the ECMS without preview has been more of an academic approach; therefore, both are used as representative "baseline" strategies.

A. Results With Simulated Terrains G1–G3

The fuel economy improvements (FEIs) with preview obtained with the ECMS or DP methods are compared with those from baseline control strategies of ECMS and RB without preview for three cruise velocities of 30, 45, and 60 mi/h. The comparisons are shown in Fig. 8.

From the simulation, we have four observations.

1) Compared with the ECMS baseline, the optimal strategy with preview yields 0.8%–20% improvement in fuel economy. Compared with the RB baseline, the improvement can even be higher and as high as 28%. The improvement is higher for G3, which is the steepest profile; in other words, the higher the root-mean-square value of grade, the better the improvement. Large improvement (up to 28%) is obtained in arc terrain G3 during a 30-mi/h cruise because of balancing the buffer of the battery and future free regeneration energy in advance. This is better shown in Fig. 9, which shows that the optimal preview solution obtained via DP is able to leave enough buffer in the battery on top of the hill in anticipation of future regeneration energy.
2) The results consistently indicate that terrain preview may be more effective at lower speeds. At higher speeds, the power demands are higher, and therefore, less regeneration opportunity is available.
3) For some simulation cases, e.g., G2, the RB baseline achieves better fuel economies than BL ECMS, which illustrates that the performance of RB control is not uniform for different simulation cases. Rule and parameters optimized for some cases are not necessarily best for others, which is a fundamental problem of the RB strategy. Based on the more consistent performance of the BL ECMS, it is expected that the improvement with respect to (w.r.t.) BL ECMS would be less than 2% over

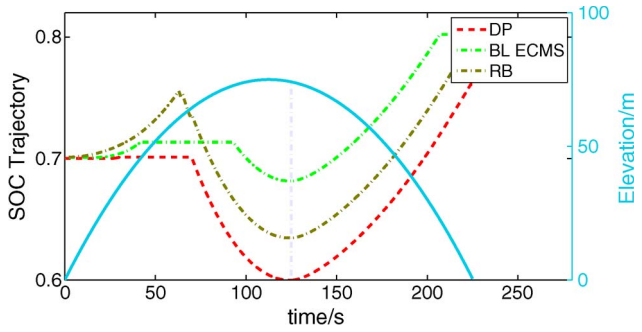

Fig. 9. Comparison of SOC trajectories for different control strategies with G3 profile and a cruise speed of 30 mi/h.

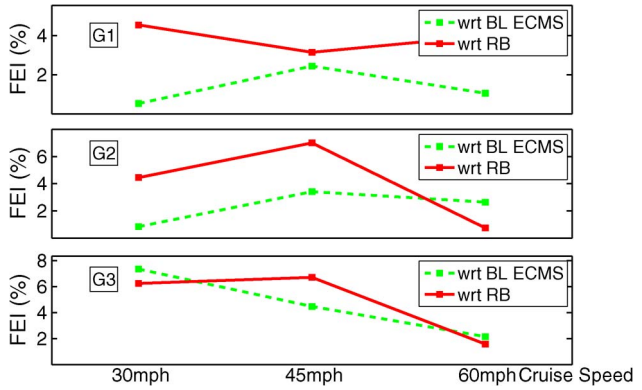

Fig. 10. FEI in arc terrains w.r.t. BL ECMS and the RB strategy with an 11-Ah battery.

arc terrains "flatter" than G1. However, the same cannot be said when the RB strategy is used as the baseline.

4) Since an important advantage of terrain preview is better utilization of battery buffer for regeneration, the improvement is expected to decrease as the size of the battery is increased. We examined this by increasing the battery size to 11 Ah from the original size of 5.5 Ah; the results in Fig. 10 confirm this expectation. Therefore, terrain preview may be an enabler for the reduction of battery size in HEVs.

B. Results With Simulated Terrains G4–G7

Grades G1–G3 represent a single hill event. To determine the average impact of preview when cruising on rolling terrain, the preceding process was repeated for real-world terrain profiles G4–G7. The information given here is summarized from the simulation results shown in Fig. 11.

1) The improvement w.r.t. BL ECMS ranges from 0.07% to 6.8%, which depends on the grade and velocity. The improvement for G4 and G5 is about or less than 2%. The improvement for G6 and G7 is about 2%–3%. The improvement is lower at higher velocities.
2) The improvement w.r.t. the RB strategy is between 0.95% and 4.2%, depending on the grade and velocity. However, the correlation between improvement and velocity is not as clear as that with BL ECMS. That means future information may be important for fuel saving, even for high speeds when the RB strategy is the baseline.
3) In all cases, the improvement at low cruising speed (30 mi/h) is significant and up to 3% or more, which

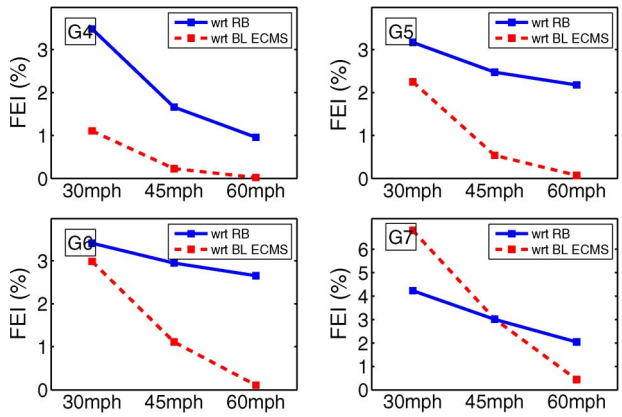

Fig. 11. FEI w.r.t. RB control and BL ECMS.

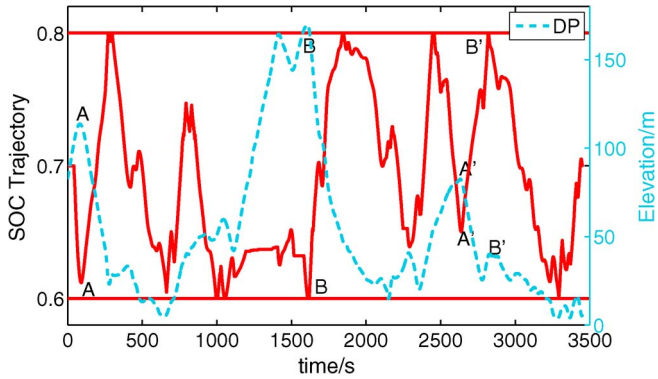

Fig. 12. SOC trajectory of DP for G7 terrain and a cruising speed of 30 mi/h. (Solid line) SOC trajectory. (Dashed line) Road elevation.

indicates that terrain preview may be more useful at low speeds.

4) Preview of long-distance downhill or steep grade profiles increases fuel savings, e.g., over terrains G6 and G7. The G6 terrain is a descending terrain, resulting in a negative average grade. Preview allows the controller to discharge the battery down and later run the engine at a higher efficiency OP to charge the battery. G7 features steep spikes in elevation, resulting in large maximum, minimum, and root-mean-square grades. Over G7, the significant change of elevation over a short interval makes large regeneration energy that can be better harnessed with the availability of terrain preview available.

C. Analysis of Power Split Behavior With and Without Preview

Terrain preview allows a more efficient operation of the powertrain by predictive planning and enables the capture of larger portions of future free regeneration energy. This behavior is illustrated in more detail in this section by a few simulation case studies.

Fig. 12 shows how predictive planning allows recuperating more energy into the battery during downhill descent. Over the G7 terrain and with a cruise speed of 30 mi/h, the DP solution anticipates the future free energy and is able to leave enough buffer, which forms the "local minimum" for SOC at points A and B on the hilltop, as shown in Fig. 12. The correlation between the "local minimum" of SOC and the top point of the hill also holds for other points, followed by a steep downhill grade, e.g., point A′. This kind of correlation becomes weak,

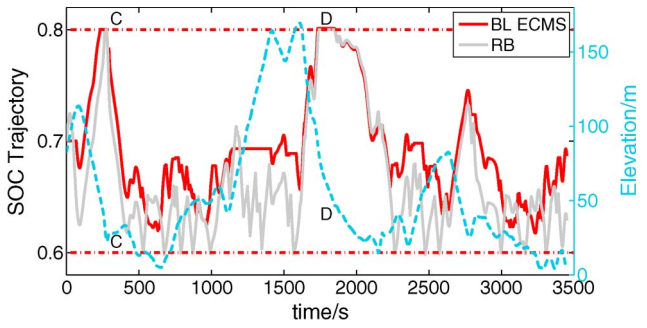

Fig. 13. SOC trajectories of BL ECMS and the RB strategy for G7 terrain and a cruising speed of 30 mi/h. (Solid line) SOC trajectory. (Dashed line) Road elevation.

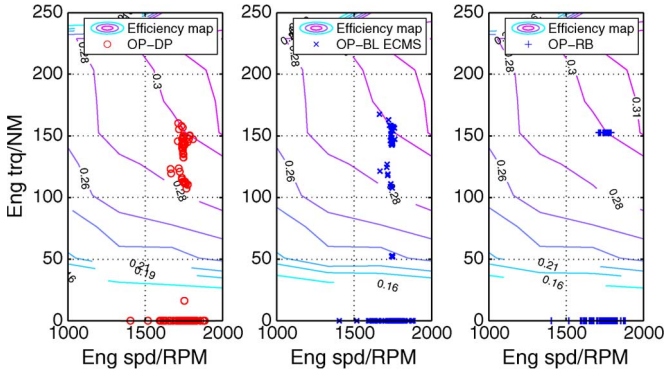

Fig. 14. Engine OP of different control strategies (DP, BL ECMS, and RB) with the G6 terrain and 30-mi/h cruise.

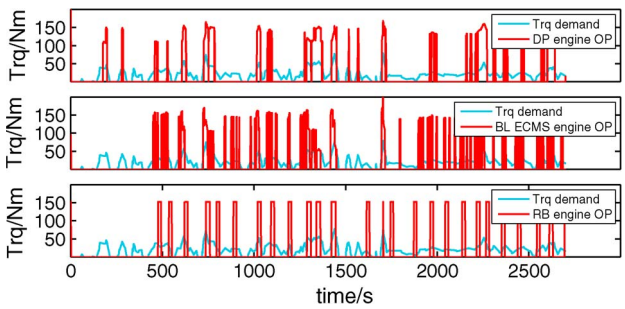

Fig. 15. Time-domain engine OP of different control strategies (DP, BL ECMS, and RB) in the case with grade G6 and a cruising speed of 30 mi/h.

disappears, or even reverses, depending on the steepness of the grade and the driver's power demand. An inverse correlation example could be seen from point B′, where the local top point of hill does not correlate with the "local minimum" but with the "local maximum" value of SOC. More examples and explanation for the "inverse correlation" are shown in Fig. 16.

BL ECMS and the RB strategy are unable to capture part of the available regeneration energy because of lack of future information. In Fig. 13, SOC trajectories for BL ECMS and the RB strategy are flat at the hill bottom points C and D because it hits the SOC's upper bound.

The engine OP is also critical for saving fuel. Figs. 14 and 15 show the engine OP in the speed-torque and torque-time planes, respectively, for the G6 terrain and cruising speed of 30 mi/h and with the DP, BL ECMS, and baseline RB strategies.

In the torque-speed plane, we observe that DP with preview and BL ECMS and the RB strategy without preview all manage

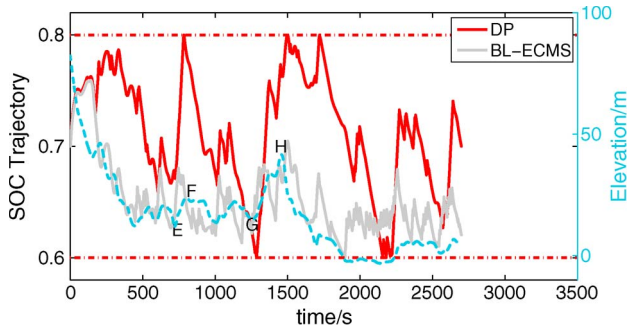

Fig. 16. SOC trajectory with different control strategies (DP and BL ECMS) in the case of grade G6 and a cruising speed of 30 mi/h. (Solid line) SOC trajectory. (Dashed line) Road elevation.

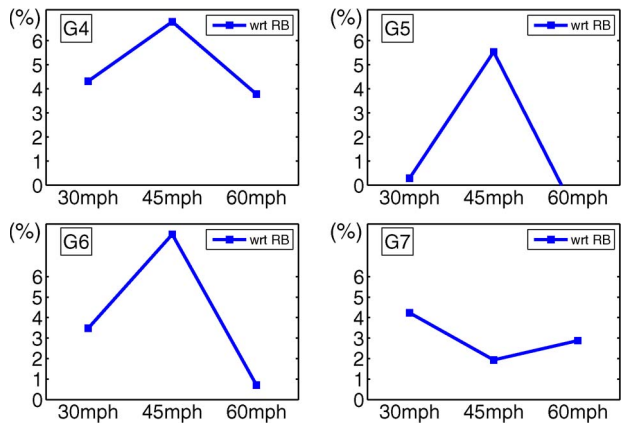

Fig. 17. Percentage increase in the battery's charging and discharging power with BL ECMS, compared with DP with preview.

to operate the engine near efficient OPs when the engine is on. The main differences between them are shown in Fig. 15 in the engine on/off timing. Due to lack of preview, BL ECMS and the RB strategy turn the engine on and off as a function of the instantaneous battery's SOC. In the lengthy downhill case of G6 terrain, the engine is less frequently turned on, and the battery is depleted to its lower bound, as shown in Fig. 16. With preview, the DP more predictively acts and charges the battery in short uphill intervals E–F and G–H, in which, due to higher torque demands, running the engine is more efficient. This results in better fuel economy of the DP approach. We note that this behavior on G6 is different from that on G7 shown earlier, where, going uphill, DP would discharge the battery. These decisions are highly dependent on the type of terrain, and the optimal power split is sometimes not intuitive.

The use of future information not only helps save fuel but may also reduce unnecessary charging and discharging of the battery. Reduced charge and discharge cycles may enhance the longevity of the battery. Figs. 17 and 18 show the percentage increase in the battery's charging and discharging power in BL ECMS and the RB strategy, respectively, compared with the case with terrain preview.

We observe that preview not only contributes to better fuel economy but also reduces the battery's charge/discharge cycles. The amount of reduction depends on the baseline control strategy: For BL ECMS, this is only a 1%–6% increase, whereas, for RB baseline, this is 50%–350% increase. In other words, the baseline RB strategy seems to aggressively discharge and

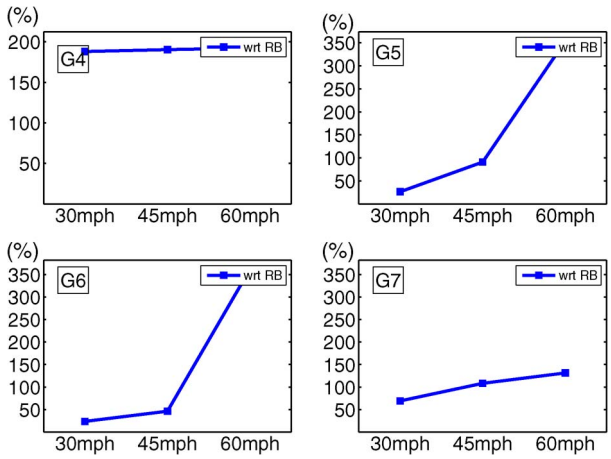

Fig. 18. Percentage increase in the battery's charging and discharging power with RB without preview, compared with DP with preview.

charge the battery to achieve good fuel economy; thus, it can have a negative influence on the battery's life. Quantifying the influence on the battery's life is an open question, which is not in the scope of this paper.

VI. Conclusion

The role of terrain preview in reducing the fuel consumption of a parallel hybrid vehicle has been investigated in this paper. To focus the study on terrain preview only, the vehicle has been assumed to cruise at a constant known velocity. Terrain preview and known velocity has made the calculation of *optimal* energy management decisions possible by solving a dynamic program or through an "optimal" ECMS. The resulting fuel economy has then been compared with that of two baseline strategies, which lacked preview: an RB strategy representative of the approach common in the industry and a modified ECMS, which is similar with the approach frequently used in academic papers. Some of the main conclusions are given here.

1) No big difference between DP and ECMS with preview is seen if the SOC trajectory does not exceed its bounds in the ECMS.
2) For most simulation cases, the ECMS baseline achieves better result than RB control. Therefore, the calculated impact of preview depends on the selected baseline strategy without preview.
3) Simulations on the hilly terrain show that an average FEI of 1%–4% is possible with terrain preview.
4) The improvement is inversely correlated to the cruising speed; i.e., it decreases at higher speeds.
5) The improvement depends on battery size. Simulation cases show that improvement decreases for a larger battery pack.
6) Preview also reduces the average energy flow to and from the battery and, therefore, may increase the battery's life.

References

[1] Powertrain System Analysis Toolkit-PSAT, Argonne Nat. Lab., Argonne, IL, 2007, Ver. 6.1
[2] B. Asadi and A. Vahidi, "Predictive use of traffic signal state for fuel saving," in *Proc. 12th IFAC Symp.Transp. Syst.*, 2009, pp. 484–489.
[3] D. P. Bertsekas, *Dynamic Programming and Optimal Control*. Belmont, MA: Athena Scientific, 2007.
[4] D. L. Buntin and J. W. Howze, "A switching logic controller for a hybrid electric/ICE vehicle," in *Proc. Amer. Control Conf.*, Seattle, WA, Jun. 1995, pp. 1169–1175.
[5] K. L. Butler, M. Ehsani, and P. Kamath, "A Matlab-based modeling and simulation package for electric and hybrid electric vehicle design," *IEEE Trans. Veh. Technol.*, vol. 48, no. 6, pp. 1770–1778, Nov. 1999.
[6] S. Delprat, T. Guerra, and J. Rimaux, "Control strategies for hybrid vehicles: Optimal control," in *Proc. IEEE 56th Veh. Technol. Conf.*, Sep. 2002, vol. 3, pp. 1681–1685.
[7] Q. Gong, Y. Li, and Z.-R. Peng, "Trip-based optimal power management of plug-in hybrid electric vehicles," *IEEE Trans. Veh. Technol.*, vol. 57, no. 6, pp. 3393–3401, Nov. 2008.
[8] L. Guzzella and A. Sciarretta, *Vehicle Propulsion Systems: Introduction to Modeling and Optimization*. New York: Springer-Verlag, 2005, pp. 190–203.
[9] W. Huang, D. M. Bevly, X. Li, and S. Schnick, "3D road geometry based optimal truck fuel economy," in *Proc. ASME Int. Mech. Eng. Congr. Expo.*, 2007, 41 695.
[10] L. Johannesson, M. Åsbogård, and B. Egardt, "Assessing the potential of predictive control for hybrid vehicle powertrains using stochastic dynamic programming," in *Proc. IEEE Conf. Intell. Transp. Syst.*, 2005, pp. 366–371.
[11] T.-S. Kim, C. Manzie, and H. Watson, "Fuel economy benefits of look-ahead capability in a mild hybrid configuration," in *Proc. 17th IFAC World Congr.*, 2008, pp. 5646–5651.
[12] A. Kleimaier and D. Schröder, "An approach for the online optimized control of a hybrid powertrain," in *Proc. 7th Int. Workshop Adv. Motion Control*, 2002, pp. 215–220.
[13] C.-C. Lin, H. Peng, J. W. Grizzle, and J.-M. Kang, "Power management strategy for a parallel hybrid electric vehicle," *IEEE Trans. Control Syst. Technol.*, vol. 11, no. 6, pp. 839–849, Nov. 2003.
[14] G. Paganelli, S. Delprat, T. Guerra, J. Rimaux, and J. Santin, "Equivalent consumption minimization strategy for parallel hybrid powertrains," in *Proc. Veh. Technol. Conf.*, 2002, vol. 4, pp. 2076–2081.
[15] P. Pisu and G. Rizzoni, "A comparative study of supervisory control strategies for hybrid electric vehicle," *IEEE Trans. Control Syst. Technol.*, vol. 15, no. 3, pp. 506–518, May 2007.
[16] G. Rizzoni, P. Pisu, and E. Calo, "Control strategies for parallel hybrid electric vehicles," in *Proc. IFAC Symp. Adv. Autom. Control*, 2004, pp. 508–513.
[17] D. Rotenberg, A. Vahidi, and I. Kolmanovsky, "Ultracapacitor assisted powertrains: Modeling, control, sizing, and the impact on fuel economy," in *Proc. Amer. Control Conf.*, 2008, pp. 981–987.
[18] M. Salman, M.-F. Chang, and J.-S. Chen, "Predictive energy management strategies for hybrid vehicles," in *Proc. IEEE Vehicle Power Propuls. Conf.*, 2005, pp. 21–25.
[19] A. Sciarretta, L. Guzzella, and M. Back, "A real-time optimal control strategy for parallel hybrid vehicles with on-board estimation of control parameters," in *Proc. IFAC Symp. Adv. Autom. Control*, 2004, pp. 502–507.
[20] A. Sciarretta, M. Back, and L. Guzzella, "Optimal control of parallel hybrid electric vehicles," *IEEE Trans. Control Syst. Technol.*, vol. 12, no. 3, pp. 352–363, May 2004.
[21] A. Sciarretta and L. Guzzella, "Control of hybrid electric vehicles," *IEEE Control Syst. Mag.*, vol. 27, no. 2, pp. 60–67, Apr. 2007.
[22] K. B. Wipke, M. R. Cuddy, and S. D. Burch, "A user-friendly advanced powertrain simulation using a combined backward/forward approach," *IEEE Trans. Veh. Technol.*, vol. 48, no. 6, pp. 1751–1761, Nov. 1999.

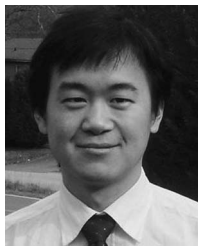

Chen Zhang received the B.S. and M.S. degrees in mechanical engineering from Chongqing University, Chongqing, China, and Shanghai Jiao Tong University, Shanghai, China, in 2003 and 2006, respectively. He is currently working toward the Ph.D. degree in mechanical engineering with the Department of Mechanical Engineering, Clemson University, Clemson, SC.

His research interests are preview-based optimal control of vehicular and energy systems.

Mr. Zhang is a Student Member of the American Society of Mechanical Engineers.

Ardalan Vahidi (M'08) received the B.S. and M.S. degrees in civil engineering from Sharif University, Tehran, Iran, in 1996 and 1998, respectively, the M.S. degree in transportation safety from George Washington University, Washington, DC, in 2002, and the Ph.D. degree in mechanical engineering from the University of Michigan, Ann Arbor, in 2005.

He is currently an Assistant Professor of mechanical engineering with the Department of Mechanical Engineering, Clemson University, Clemson, SC. His current research interests are optimization-based control methods and the control of vehicular and energy systems.

Dr. Vahidi is a member of the American Society of Mechanical Engineers and the Society of Automotive Engineers.

Pierluigi Pisu (M'07) received the Ph.D. degree in electrical engineering from The Ohio State University, Columbus, in 2002.

He is currently an Assistant Professor with the Department of Mechanical Engineering, Clemson University, Clemson, SC. He was the holder of two U.S. patents in area of model-based fault detection and isolation. His research interests are fault diagnosis with application to vehicle systems, energy management control of hybrid electric vehicles, and sliding mode and robust control.

Dr. Pisu is a member of the American Society of Mechanical Engineers and the Society of Automotive Engineers. He was the recipient of the 2000 Outstanding Ph.D. Student Award from The Ohio State University Chapter of the Honor Society Phi Kappa Phi and the 2005 Rolls-Royce Scholarship Award for demonstrated leadership, communication, teamwork, and academic excellence. He is a 2009 Honored Member of *Biltmore Who's Who* and a 2004 Honored Member of *Strathmore's Who's Who*.

Xiaopeng Li received the B.Eng. (Hons.) and M.Eng. degrees in geomatics engineering from Wuhan University, Wuhan, China, in 1985 and 1989, respectively, and the Ph.D. degree in remote sensing from the University of New Brunswick, Fredericton, NB, Canada, in 1999.

Since early 1999, he has been with Intermap Technology Corporation, Ottawa, ON, Canada, where he is currently a Core Component Manager within the Automotive Division.

Dr. Li is a member of the Society of Automotive Engineers International.

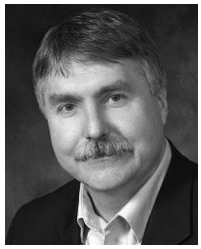

Keith Tennant received the B.Sc. degree in electrical engineering from the University of Calgary, Calgary, Canada.

He is a Professional Engineer and is currently the Director of Customer Care with the Intermap Technology Corporation, Ottawa, ON, Canada. Since 1987, he has been involved in remote sensing and mapping activities. He has contributed both as an engineer, designing radar-based remote-sensing systems, and as a manager, organizing and overseeing large-scale mapping operations on five continents. He has recently been applying this experience in support of novel applications of mapping information for the automotive industry. This support includes university and industry research of mapping data as a predictive sensor within the transportation industry.